

# Noninvasive detection of counterfeited ampoules of dexamethasone using NIR with confirmation by HPLC-DAD-MS and CE-UV methods

Oxana Rodionova · Alexey Pomerantsev ·  
Lars Houmøller · Alexey Shpak · Oleg Shpigun

Received: 15 December 2009 / Revised: 28 February 2010 / Accepted: 29 March 2010 / Published online: 29 April 2010  
© Springer-Verlag 2010

**Abstract** Application of near-infrared (NIR) measurements together with chemometric data processing is widely used for counterfeit drug detection. The most difficult counterfeits to detect are the “high quality fakes”, which have the proper composition but are produced in violation of technological regulations by underground manufacturers. This study uses such forgeries and addresses important issues. The first is the possibility of applying the NIR/chemometric approach to the detection of injectable formulations of drugs (in this case dexamethasone), which are aqueous solutions with low concentration of active ingredients, directly in the closed ampoules. The second issue is the comparison of NIR/chemometric conclusions with detailed chemical analysis.

**Keywords** High quality forgeries · PCA · NIR · HPLC-DAD-MS · CE-UV

---

O. Rodionova (✉) · A. Pomerantsev  
Institute of Chemical Physics RAS,  
Kosygin str. 4,  
119991 Moscow, Russia  
e-mail: rcs@chph.ras.ru

A. Pomerantsev  
State South Research & Testing Site RAS,  
Teatral'naya 8a,  
354000 Sochi, Russia

L. Houmøller  
Arla Foods amba,  
Sønderupvej 26,  
6920 Videbæk, Denmark

A. Shpak · O. Shpigun  
Moscow State University,  
119991 Moscow, Russia

## Introduction

Rapid and reliable analytical methods for counterfeit drug detection are of great importance. Numerous medical publications report on the ‘clever’ forgeries that constitute a growing hazard to public health. In 2006, the World Health Organization established a partnership called International Medical Product Anti-Counterfeiting Taskforce (IMPACT) [1, 2]. At the first IMPACT meeting it was claimed that: “no country is free of this problem, which plagues developing and developed countries alike.” Moreover it was stated that: “counterfeit drugs are on the verge of becoming a silent pandemic.” Presently, drug counterfeiting is becoming more and more sophisticated. The fake medications are produced by using modern pharmaceutical equipment; they contain a proper amount of the active ingredient; and the packages are of excellent printing quality. Therefore some forgeries can only be revealed by a complex analysis of excipients, which are inactive substances present in a drug.

Nowadays the conventional analytical methods (GC, HPLC, MS, etc.) applied in pharmacopeia are often replaced with an alternative approach which combines near-infrared (NIR) spectroscopy with chemometric multivariate data analysis (MDA). This is a very rapid method and several research groups [3–8] reported on the promising results achieved with this technique. Typically, MDA can clearly distinguish the genuine and counterfeited samples, placing them in different areas in the scores plot, or in the residual/leverage plot, etc. But MDA cannot explain the reasons for such discrimination because an NIR spectrum does not contain separated peaks but combination bands and overtones which cannot be interpreted in terms of impurities or concentrations without prior calibration. Therefore some researchers do not rely on such types of analysis.

In this work we attempt to verify and explain the chemometrics-driven conclusions by comparison with a complex chemical analysis. The research is based on the case study of injection of dexamethasone, which is a glucocorticosteroid. The manufacturer detected a batch of suspected counterfeit medicine available on the market by revealing the lack of several printing marks, which are hidden in the package for security reasons. However, the standard pharmacopoeia tests performed at the manufacturer's facility did not confirm the counterfeiting since the quality and quantity of the active substance was within the standards. Later the suspicious drug and genuine samples with identical batch numbers were subjected to the NIR-based analysis.

The main obstacle in NIR spectroscopy analysis is the strong water absorption bands (around  $5,000\text{ cm}^{-1}$  and  $7,000\text{ cm}^{-1}$ ) that conceal the net analytic signal from the drug ingredients. As the NIR/chemometrics approach cannot at present clarify the origins of counterfeiting (insufficient quantity of excipient, or presence of odd impurities, etc.), we decided to perform additional experiments employing a wide range of modern analytical methods, such as GS-MS, HPLC-DAD-MS, and CE-UV, which are able to give the answers to such questions.

The objectives of the presented study are summarized as follows:

1. To introduce a special approach to the through-ampoule NIR measurements of aqueous solutions having low concentration of ingredients.
2. To demonstrate a chemometric technique employed in counterfeit detection
3. To compare the results obtained by the conventional analytical methods with the chemometrics-based conclusions.

## Samples

A 4% aqueous solution of dexamethasone 21-phosphate was present in closed transparent glass ampoules. Each ampoule contained 1 ml. Two batches of genuine ampoules, called G1 and G2, and one batch of counterfeit ampoules, called F2, were studied. Each batch contained 15 ampoules. Batches G2 and F2 had identical production times and series labels: the difference was recognized by secret printing on the packages.

## Methods

### Near-infrared (NIR) measurements

NIR spectra were acquired in the wavenumber interval  $5,380\text{--}11,000\text{ cm}^{-1}$  with a resolution of  $8\text{ cm}^{-1}$  on an ABB

Bomem MB160 spectrometer equipped with a thermoelectrically cooled InAs detector. The ampoules were placed upside down in an 8-mm vial holder held at  $30\text{ }^\circ\text{C}$ . For background spectrum, 100 scans of the empty vial holder were used, and a 1% transmission filter was used to attenuate the signal. For the sample spectra, a 3.2% filter and 50 scans were used. The gain setting was A (no amplification) for the background spectrum and C (4 times amplification) for the sample spectra. A total of 45 ampoules from three batches were measured in transmittance mode. The raw spectra are shown in Fig. 1 (left).

Two regions with strong water absorption bands centered around  $5,000\text{ cm}^{-1}$  and  $7,000\text{ cm}^{-1}$  were excluded from the analysis. The range above  $9,000\text{ cm}^{-1}$  does not carry any useful information and was also excluded. As a result, two informative ranges were employed:  $5,500\text{--}6,400\text{ cm}^{-1}$  and  $7,200\text{--}9,000\text{ cm}^{-1}$  (703 wavenumbers).

### Data pretreatment

To decrease light scattering and other sources of variation that are not related to the chemical information, raw spectra should be preprocessed before further data analysis. We applied the standard normal variate (SNV) method [9] which centers and scales individual spectra as follows

$$\tilde{x}_{ij} = (x_{ij} - \bar{x}_i) / s_i \quad (1)$$

where  $x_{ij}$  is the spectral measurement at the  $j$ -th wavenumber for the  $i$ -th sample,  $\bar{x}_i$  is the mean value for  $i$ -th spectrum,  $s_i$  is the standard deviation of the same spectrum, and  $\tilde{x}_{ij}$  is the corresponding corrected value. The effect of transformation (1) is very similar to multiplicative scatter correction [9], but SNV treats each spectrum individually and does not use the mean value of any set.

SNV transformation was applied for the investigated spectra in the combined range  $5,500\text{--}6,400\text{ cm}^{-1}$  and  $7,200\text{--}9,000\text{ cm}^{-1}$ . The results of the pretreatment are shown in Fig. 1 (right). These SNV preprocessed data were further used for chemometric analysis.

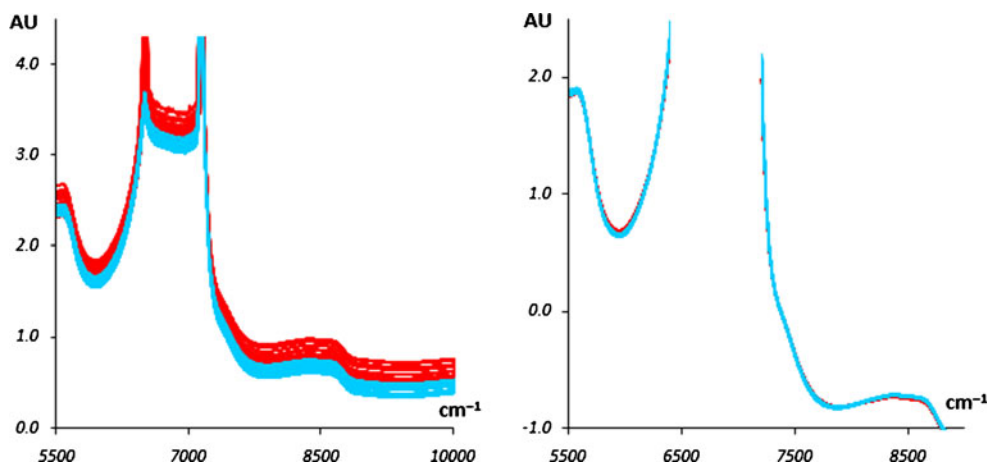
### Chemometrics

Data sets with many variables can be simplified through variable reduction and thereby be more easily interpreted. Principal component analysis (PCA) [10] is a well-known variable reduction technique, in which the spectral matrix  $\mathbf{X}$  is decomposed as

$$\mathbf{X} = \mathbf{TP}^t + \mathbf{E}, \quad (2)$$

Here  $\mathbf{X}$  is the  $I \times J$  data matrix,  $\mathbf{T}$  is the  $I \times A$  matrix of score vectors, where score vectors  $\mathbf{t}_a$  are orthogonal, i.e.,

**Fig. 1** NIR measurements of 30 genuine samples (blue lines) and 15 fakes (red lines). Left raw spectra, right spectra after standard normal variate (SNV) pre-processing



$\mathbf{T}^t \mathbf{T} = \text{diag}(\lambda_a)$ , and  $\lambda_a$  are eigenvalues of matrix  $\mathbf{X}^t \mathbf{X}$ .  $\mathbf{P}$  is the  $J \times A$  matrix of loading vectors,  $\mathbf{E}$  the  $I \times J$  residual matrix,  $I$  the number of objects,  $J$  the number of variables (which in our case is the number of wavenumbers), and  $A$  is the number of components calculated (i.e., principal components, PCs).

Two important characteristics of the PCA model with respect to each calibration object can be defined. They are the score distance (SD) and the orthogonal distance (OD). For a given number of principal components,  $A$ , the SD,  $h_i$  is compared with the average SD,  $h_0$

$$h_i = \mathbf{t}_i^t (\mathbf{T}_A^t \mathbf{T}_A)^{-1} \mathbf{t}_i = \sum_{a=1}^A \frac{t_{ia}^2}{\lambda_a}, \quad i = 1, \dots, I, \quad (3)$$

$$h_0 = \frac{1}{I} \sum_{i=1}^I h_i \equiv \frac{A}{I}$$

The OD,  $v_i$ , is calculated as the sum of the squared residuals presented in matrix  $\mathbf{E} = \{e_{ij}\}$  and compared with the average OD  $v_0$ ,

$$v_i = \sum_{j=1}^J e_{ij}^2, \quad v_0 = \frac{1}{I} \sum_{i=1}^I v_i. \quad (4)$$

Soft independent modeling of class analogy (SIMCA) is a supervised pattern recognition method [11]. The idea behind this method is that each group of objects is independently subjected to PCA with its own complexity (the number of PCs) and the acceptance area for each model is defined. In this study we applied a modified SIMCA approach that was earlier presented by one of the authors [12]. This approach is based on the following principles.

1. It is supposed that both the SD and OD values are chi-square distributed, namely

$$\frac{h}{h_0} \propto \frac{1}{N_h} \chi^2(N_h) \quad \frac{v}{v_0} \propto \frac{1}{N_v} \chi^2(N_v). \quad (5)$$

2. These chi-squared distributions depend on parameters  $N_h$  and  $N_v$  that are the numbers of degrees of freedom (DoF). Their values are not derived from theoretical considerations, but estimated from the calibration set, employing values  $h_i$  and  $v_i$ ,  $i=1, \dots, I$ .
3. For the construction of the acceptance area, a well-known equation

$$N_h \frac{h}{h_0} + N_v \frac{v}{v_0} \propto \chi^2(N_h + N_v) \quad (6)$$

is used. For a given type I error  $\gamma$ , it provides an acceptance area, examples of which are presented in Fig. 3.

#### GC-MS

The experiments were carried out on a 6890 N gas chromatograph equipped with a 5973 N mass-selective detector with an electron-impact ionization source (Agilent Technologies, Germany). The separation was performed on a chromatographic column HP-INNOWAX, 30 m  $\times$  25 mm  $\times$  0.25 mm (Agilent Technologies, Germany). Helium at a flow rate of 1 ml/min was used as the mobile phase. The amount of injected sample was 1  $\mu$ l in splitless mode for organic samples and 1  $\mu$ l in split mode (1:3) for water samples. The temperature gradient profile was as follows: 40  $^\circ$ C for 10 min, 40–220  $^\circ$ C at 10  $^\circ$ C/min, 220  $^\circ$ C for 5 min, 220–40  $^\circ$ C at 10  $^\circ$ C/min, 40  $^\circ$ C for 10 min. The inlet and detector temperatures were 180  $^\circ$ C and 200  $^\circ$ C respectively. The detection was performed in scan mode in the  $m/z$  range from 30 to 350.

The identification of the compounds was carried out by using a NIST 2005  $^\circ$  database.

#### HPLC-DAD-MS

The chromatographic system Agilent 1100 (Agilent Technologies), equipped with binary gradient pump,

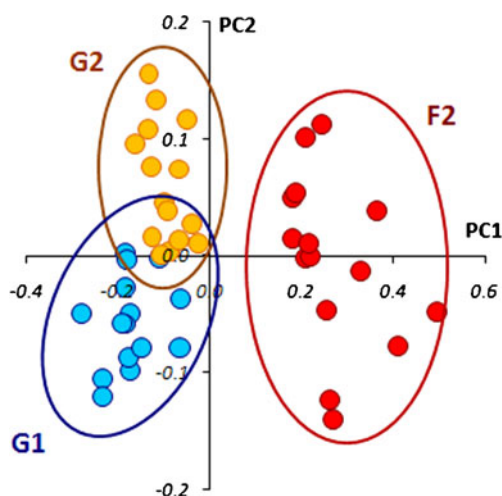


**Fig. 2** PCA score plot (PC2 vs. PC1); overview of total dataset (45 samples)

mobile phase degasser, autosampler, column thermostat, and diode-array and mass-selective detectors was used for the experiments. The chromatographic column was a Luna C18, 250×4.6 mm, 4 μm (Phenomenex, USA), and the mobile phase consisted of a 2 mM ammonia acetate buffer (solvent A) and acetonitrile (solvent B) mixture. The separation was achieved at 30 °C at a flow rate of 0.5 ml/min by the following gradient profile: 0–6 min 100% A; 20–25 min 90%B, 25.1–30 min 100% A. The sample volume was 50 μl. The spectrophotometric detection was conducted at 210, 254, 275, and 360 nm simultaneously. The mass-selective detection was carried out by using an electrospray ionization mode. Positive ions in the  $m/z$  range from 100 to 500 were collected. The fragmentor voltage was 100 V. The parameters of the ionization chamber were taken from the tune file (drying

gas velocity 12 l/min, temperature of the gas 350 °C, capillary voltage 3 kV).

#### CE-UV

The experiments were performed on a Capel 105 M electrophoresis system (Lumex, St Petersburg, Russia) connected to a MultiChrom 1.56 data acquisition system (Ampersend, Moscow, Russia). The standard fused-silica capillary, 60 cm×75-μm i.d., with a detection window at 50 cm, was used. The buffer consisted of 10 mM sodium tetraborate and 40 mM sodium dodecylsulphate. The voltage was 25 kV. The capillary was thermostated at 25 °C. Detection at 254 nm was used. All samples were injected hydrodynamically (30 mbar, 5 s).

#### Chemicals and sample pretreatment

Sodium tetraborate, sodium dodecylsulphate, and ammonia acetate were purchased from Sigma Aldrich (USA). Organic solvents such as methylene chloride and acetonitrile were obtained from Panreac (Spain). Water used in the experiments had a resistance of 18.2 mΩ or better.

For the GC-MS analysis, 200 μl of methylene chloride was added to 400 μl of the investigated sample, the mixture was thoroughly mixed and centrifuged at 3,000 rpm for 2 min, and the organic layer was separated. The aqueous and organic phases were analyzed separately. Additionally, the sample was evaporated at room temperature till 50 μl and the organic layer was analyzed once more.

To analyze the samples by the HPLC method, no special procedure of sample pretreatment was necessary. The aqueous solutions under investigation were directly injected into the chromatographic system.

For the CE-UV analysis the original solution was diluted twice with water.

**Fig. 3** Classification plots. Axes are square root transformed for better appearance. *Left* modeling set (squares) G1 blue; classification set (circles) G2 yellow, F2 red. *Right* modeling set (squares) G1 blue, G2 yellow; classification set (circles) G1 blue, G2 yellow, F2 red

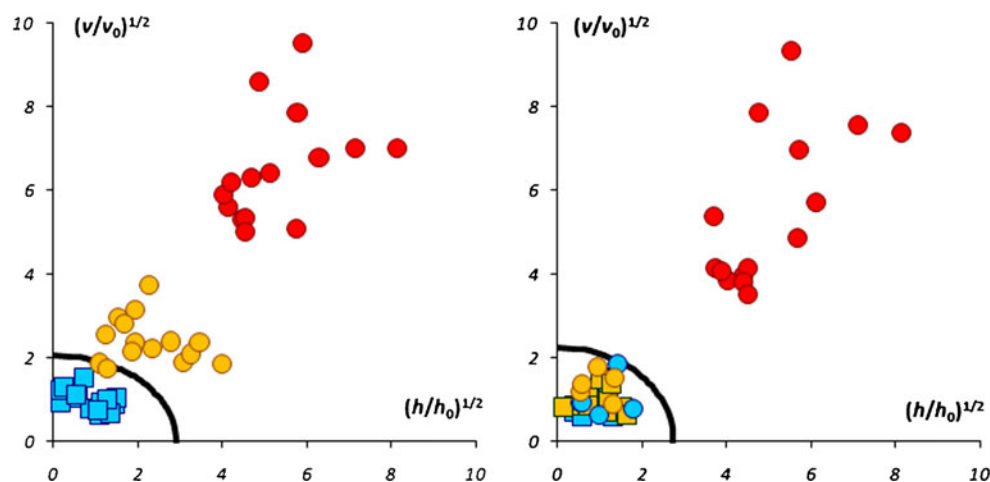


**Table 1** Average values for peak characteristics with relative standard deviations (RSDs) for the impurities in genuine samples, four replicates

Impurity no.	Retention time (min)	Peak area (a.u.)	Peak height (mAU)	RSD, %		
				<i>t</i>	<i>S</i>	<i>h</i>
1	17.23	367.1	97.93	0.10	7.71	8.26
2	20.11	62.5	13.50	0.90	23.20	7.91
3	20.24	76.6	16.35	1.01	13.67	5.39
4	22.89	557.1	92.08	0.12	0.97	1.90
5	23.07	44.1	7.23	0.11	4.77	3.46
6	23.49	26.9	4.85	0.11	10.02	6.41
7	23.78	28.0	4.60	0.08	26.81	25.91
8	24.08	103.4	10.23	0.09	22.35	19.29
9	24.83	1226.9	174.05	0.11	0.51	1.50

HPLC-DAD, UV detection at 254 nm

*a.u.* arbitrary units, *AU* absorbance units

## Results and discussion

### NIR measurements with chemometric data processing

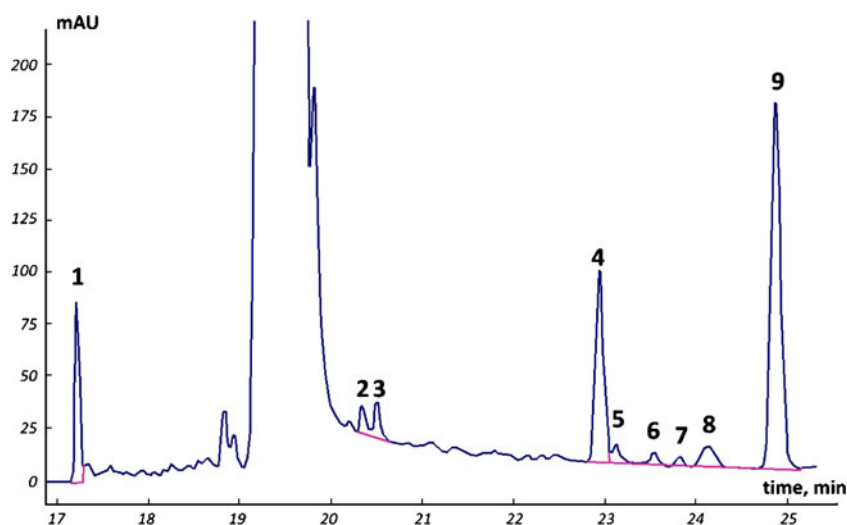
The explorative PCA analysis on the whole dataset, 45 ampoules, showed an essential difference between F and G samples and some tendency for clustering between G1 and G2 groups in the PC1/PC2 score plot (Fig. 2). The PCA model explained 95% of total *X*-variance.

Afterwards, only one set of genuine ampoules, G1, was used for modeling and sets G2 and F2 were used as “new” samples for classification. The corresponding PCA model with two PCs explained 91% of total variance. Numbers of degrees of freedom for the SDs and ODs were calculated as  $N_h=2$  and  $N_v=4$  respectively. SIMCA was applied with  $\gamma=0.01$  for type I error.

The classification plot showed that two samples in class G2 fitted the model of class G1 and other samples in class G2 were located very close to the acceptance area. All samples in class F2 were located far from the

class G1 acceptance area (Fig. 3, left). Similar classification results (not shown here) were obtained in the case where the set G2 was used for modeling and the sets G1 and F2 were classified by using the model of class G2.

This analysis showed that samples from sets G1 and G2 were similar but not identical and that in modeling of the genuine sample class the natural batch-to-batch variation should be taken into account. For this purpose ten samples from set G1 and ten samples from set G2 were selected as a modeling set and the rest (5 from G1, 5 from G2, and 15 from F2) were used for classification. This PCA model (genuine) with two PCs explained 93% of total variance. DoFs for this model were  $N_h=2$  and  $N_v=3$ ,  $\gamma=0.01$ . The corresponding SIMCA plot is presented in Fig. 3 (right). This Figure shows that all samples were classified adequately. Objects from sets G1 and G2 were properly classified as genuine, and samples from set F2 were located far beyond the acceptance area for the genuine model.

**Fig. 4** The integrated HPLC-DAD chromatogram of the genuine sample G1 (at 254 nm)

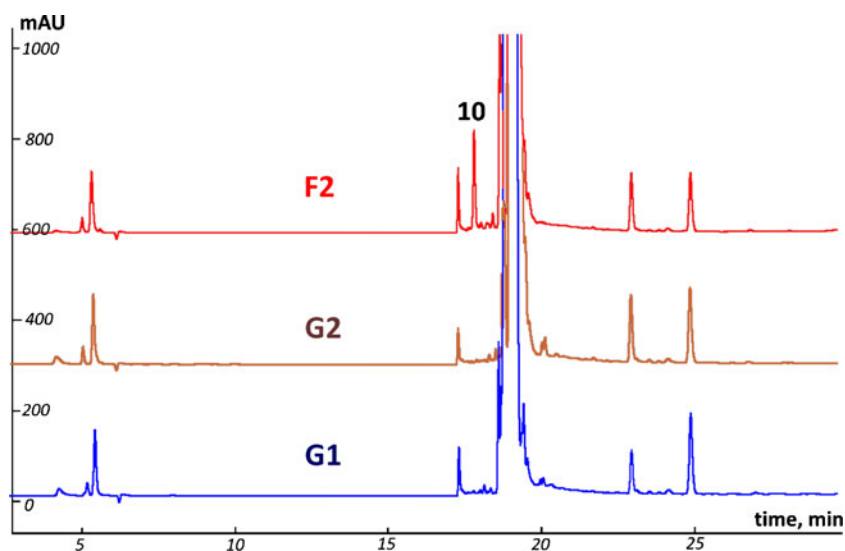


**Fig. 5** HPLC-DAD chromatograms of the fake (F2) and genuine (G2 and G1) samples. UV detection at 254 nm. The chromatograms for F2 and G2 have been displaced for clarity

It should be stressed that application of a PCA model with few components was determined by the SIMCA approach, as the goal is to model only common properties of each class rather than intrinsic sample individualities.

The following conclusions could be drawn from the chemometric study:

1. Set F2 was distinct from both sets G1 and G2
2. Sets G1 and G2 were similar, but distinguishable

For reliable discrimination between genuine and counterfeit samples it is necessary to use a modeling set including samples from various batches.

The path length of the NIR light through the top of the ampoules was such that the absorbance was very

high (also resulting in saturation of the detector at the water peaks). This means that the technique was able to detect small differences in the samples. With the present instrumentation and setup it seems plausible that the successful discrimination originated from chemical differences detected by the sensitive measurements. Wet-chemistry experiments presented below confirmed this assumption.

#### GC-MS

The samples were subjected to GC-MS analysis with two types of sample preparation. No differences between genuine and fake samples were found. The composition of the samples as well as the amounts of the discovered

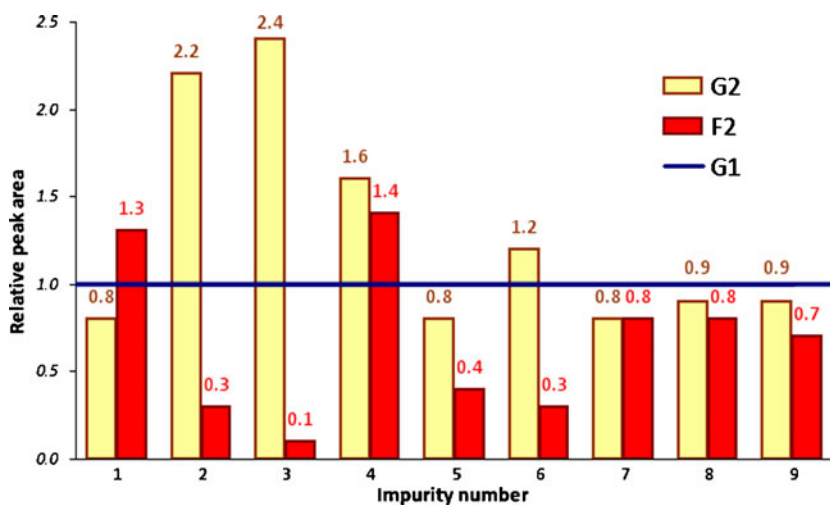


**Fig. 6** Peak areas of the impurities (HPLC-DAD, UV detection at 254 nm). The genuine G1 sample is used as the reference

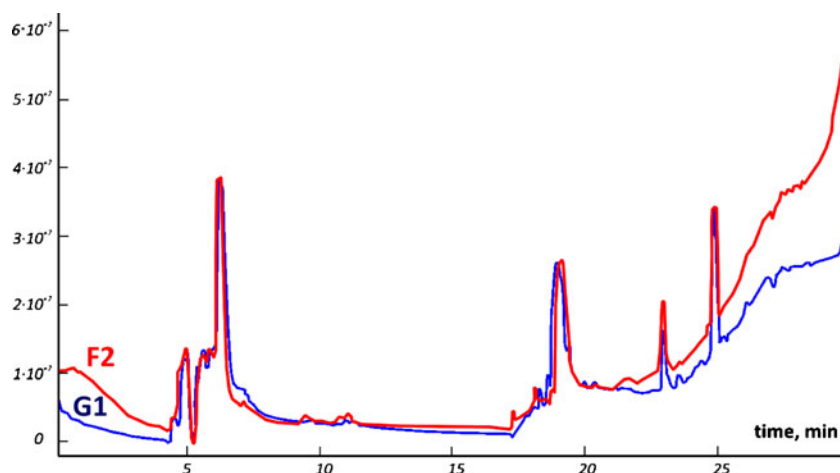


**Fig. 7** HPLC-MS TIC chromatograms of the genuine G1 and fake F2 samples

components was identical, i.e., the GC-MS method did not allow for discriminating fake and original samples.

#### HPLC-DAD

To investigate the repeatability of the method, the genuine sample G1 was injected into the chromatographic system four times. This experiment showed that the retention times of the microimpurities were very stable (see Table 1), and in this case, if any other impurities were present in the sample, they could be easily discovered with this method. Retention times and the areas of the impurities peaks were calculated according to the scheme of integration shown in Fig. 4 at 254 nm.

The relative standard deviation (RSD) was calculated for the retention time, peak area, and peak height of nine impurities (Table 1).

The RSD for the retention time did not exceed 0.1% for the impurities 1 and 4–9 which may be considered as a very stable result. Moreover, the RSD for the peak area was low

for the impurities 1, 4, and 9. Because of these results, it was possible not only to determine the number of the impurities present in the sample, but also to calculate their relative amounts.

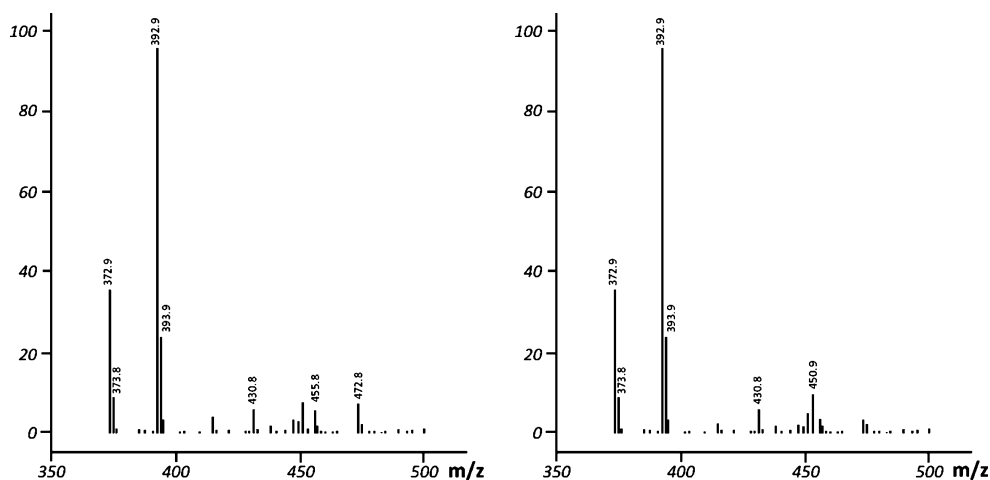
Chromatograms of the fake (F2) and the genuine (G2 and G1) samples are shown in Fig. 5.

Figure 5 presents a large peak with the retention time 17.72 min in the chromatogram of the fake sample (impurity 10) and the absence of impurities 2 and 3. Peaks of all other impurities are practically identical, and their retention times are in good agreement.

Relative peak areas with the genuine (G1) sample as the reference are presented in Fig. 6.

This comparison showed that the composition of microimpurities in samples from batches G1 and G2 were identical but for some of impurities, especially for nos. 2–4, they differed in quantity. The fake sample had very low quantities of impurities 2 and 3, and impurity 10 was not found in genuine samples. The most representative results were obtained at the wavelength 254 nm for the diode-array detector (Fig. 5), but at the

**Fig. 8** HPLC-MS spectrum of the impurity 4. *Left* the genuine G1 sample, *right* the fake (F2) sample



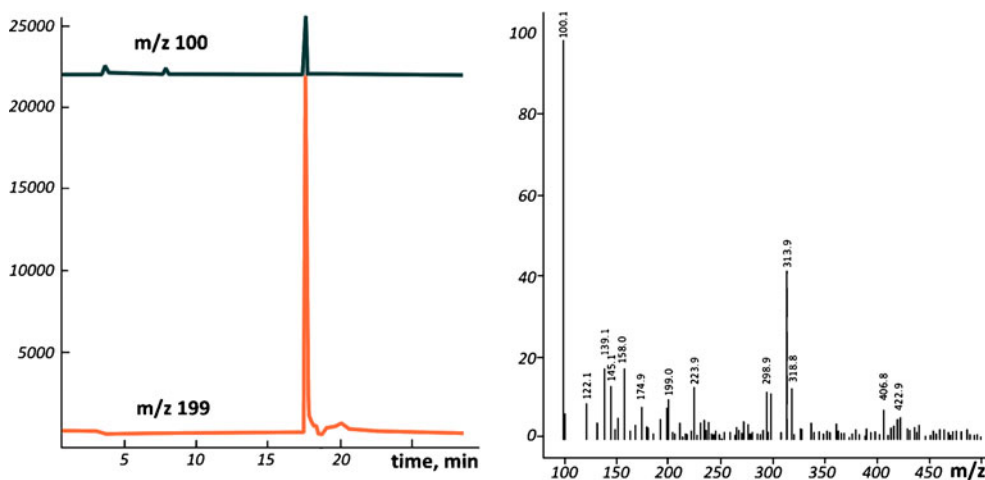


**Fig. 9** HPLC-MS chromatogram of the fake sample. *Left* selected ion mode,  $m/z$  100 and 199. The  $m/z=100$  trace has been displaced for clarity. *Right* mass spectrum of impurity 10 (retention time 18.08 min)

other wavelengths impurity 10 in the fake sample was also discovered, and the retention time of this compound was exactly the same.

#### HPLC-MS

The mass spectra of all ten impurities, discovered by using UV detection, were studied, and mass chromatograms in total ion current (TIC) mode were also compared to discover any possible additional differences between fake and genuine samples (Fig. 7).

A good agreement between chromatographic profiles in general and mass spectra of different peaks in particular was found. For example, mass spectra of the impurity 4 (retention time 22.89 min) were very similar for the genuine and fake samples (Fig. 8)

As in the case of using HPLC-DAD, differences between genuine and fake samples were also found by application of HPLC-MS, including impurity no. 10 (Fig. 9)

The retention time of this compound was in agreement with the retention time of impurity 10 discovered by using the diode-array detector. The difference between the times of the peak maxima (17.72 and 18.08 min) was caused by the distance between diode-array and mass-selective detectors. In general the results of the HPLC-MS technique agreed with those obtained by using the diode-array detection and can be used for solving the task under consideration.

#### CE-UV

The electropherograms of the fake and genuine samples are shown in Fig. 10.

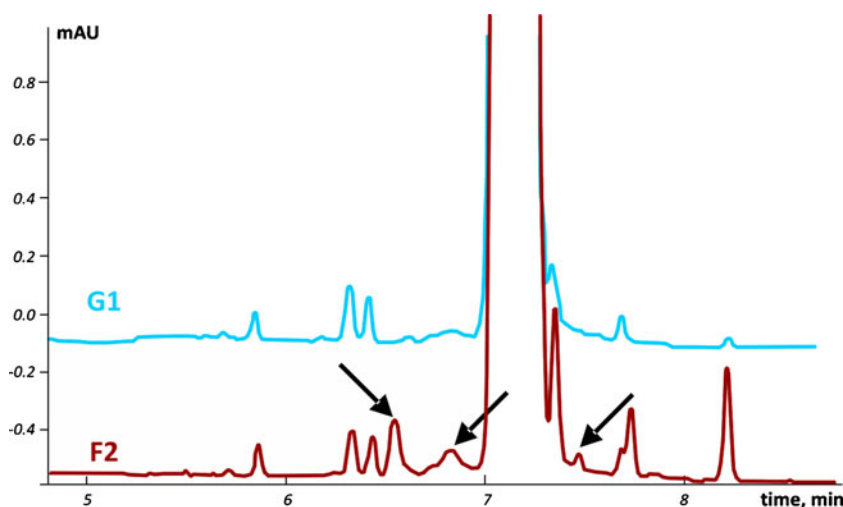


**Fig. 10** CE electropherograms of the genuine (G1) and fake (F2) samples. The G1 trace has been displaced for clarity. Impurities present in F2 but not in G1 are marked

Capillary electrophoresis reliably found four impurities (Fig. 10) in the fake sample, which were not present in the genuine sample. This was due to the higher efficiency of separation and special selectivity of the CE-UV method. Thus the capillary electrophoresis method showed the most informative results for discrimination among the analytical methods when samples were close in their chemical compositions.

## Conclusions

The GC-MS method, which is prescribed to be used as a standard method in pharmacopeia, did not find any significant differences between genuine and fake samples.

HPLC-UV chromatograms showed a large peak, corresponding to impurity 10, for the fake sample, which, together with the absence of impurities 2 and 3, makes it possible to detect forgery. Peak positions for samples G1 and G2 were identical, but for impurities 2–4 peak areas they differed notably.

HPLC-MS also revealed an impurity, which was absent in the genuine samples. As in the case of the UV detection results, MS detection provides the possibility for discrimination of fake and genuine samples.

The CE-UV method confirmed the presence of four additional impurities in the fake sample.

The results of the NIR tests were completely confirmed by the intensive chemical studies. Samples from batches G1 and G2 were similar in their impurity composition but differed in the quantity of the impurities. Most probably this can be considered as ordinary batch-to-batch variation. Therefore, a reliable model should be based on samples from different batches. Differences in impurity composition are reflected in NIR spectra and help to disclose fake samples. NIR measurements with chemometric data processing provides a quick and easy procedure for discrimination between genuine and fake drugs even in cases when forgery is “of high quality” and has a content very similar to genuine samples, and when standard pharmaceutical tests cannot recognize forgery. In this work

drugs for injection were studied. Such kinds of drugs are aqueous solutions with low concentrations of active substances and excipients. To be able to analyze such objects reliably by NIR measurements the pertinent instrumentation setup should be used.

Microimpurity analysis is important for disclosure of “high quality forgeries” as impurity composition carries important information not only about the product itself but also about the manufacturing process, i.e., differences in equipment materials, which can be used as fingerprints for the medicine even in the case when identical raw materials are applied. NIR measurements together with multivariate data analysis can be used for monitoring of big batches of products. However, NIR analysis cannot reveal the sources of disagreement between the tested samples. Therefore the suspicious samples should afterwards be subjected to detailed chemical analysis.

## References

1. IMPACT—International Medical Product Anti-Counterfeiting Taskforce (2009) <http://www.who.int/impact/en/>. Accessed 10 Oct 2009
2. WHO (2006) Combating counterfeit drugs: a concept paper for effective international collaboration. <http://www.who.int/medicines/events/FINALBACKPAPER.pdf>. Accessed 10 Oct 2009
3. Blanco M, Villarroya I (2002) *TrAC* 21:240–250
4. Trafford AD, Jee RD, Moffat AC, Graham P (1999) *Analyst* 124:163–167
5. Henrique Frasson Scafì S, Pasquini C (2001) *Analyst* 126:2218–2222
6. Rodionova OY, Houmøller LP, Pomerantsev AL, Geladi P, Burger J, Dorofeyev VL, Arzamazstsev AP (2005) *Anal Chim Acta* 549:151–158
7. Yoon WL (2005) *Am Pharm Rev* 8:115–118
8. Ricci C, Eliasson C, MacLeod NA, Newton PN, Matousek P, Kazarian SG (2007) *Anal Bioanal Chem* 389:1525–1532
9. Næs T, Isaksson T, Fearn T, Davies T (2002) *Multivariate calibration and classification. NIR*, Chichester
10. Martens H, Naes T (1998) *Multivariate calibration*. Wiley, New York
11. Wold S (1976) *Pattern Recognit* 8:127–139
12. Pomerantsev AL (2008) *J Chemom* 22:601–609